21st Australasian Fluid Mechanics Conference
Adelaide, Australia
10-13 December 2018

Using Radiative Heating to Perform Fluid-Thermal-Structural Interaction Experiments in a Short-Duration Hypersonic Wind Tunnel

A.J. Neely[1], G.M.D. Currao[1] and L.P. McQuellin[1]

[1]School of Engineering and Information Technology
UNSW Canberra, 2600, Australia

Abstract

This work discusses the design and implementation of close-proximity radiative heaters for aerothermoelastic experiments in short-duration hypersonic facilities. The radiators are employed to selectively heat a compliant panel both to a specific temperature and to impose a prescribed thermal spatial distribution. Analytical and numerical models are used to demonstrate the performance of these radiators. The analytical study shows that the temperature of the test panel is primarily a function of the panel thickness and the proximity of the heater. A 3D finite element study confirmed these predictions and found that reasonable temperature uniformity could be achieved on the compliant panel ($\Delta T < 60$ K for $T_{max} = 550$ K) for practical arrangements. FEM simulations also demonstrated that non-uniform temperature distributions can be prescribed on the panel through use of a nonuniform heater but that these distributions are smeared both by thermal conduction in the panel and radiative crosstalk in the panel-heater gap.

Introduction

Hypersonic flight is unavoidably associated with extreme convective heating loads which can result in significantly elevated structural temperatures. This has a magnified effect on the vehicle skin-panels of semi-monocoque designs, which are generally favoured for hypersonic aircraft. These high temperatures will influence the flow field [1,8], degrade the mechanical properties of the structure and potentially deform the structure via buckling. All of these phenomena will influence the resulting severity of any fluid-structure interactions (FSI) induced by pressure differentials, boundary layer and boundary layer transition effects and shock boundary layer interactions. Thus this fluid-thermal-structural coupling will influence the lifing of hypersonic skin panels [3,14] and therefore requires accurate modelling.

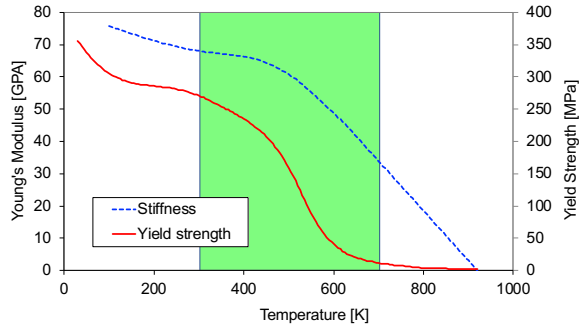

Figure 1. Variation in stiffness and strength with temperature for aluminium alloy 6061-T6. [18]

The mechanical properties of metal alloys deteriorate with elevated temperatures [18]. The properties central to the fluid-thermal-structural interaction (FTSI) behaviour of an airframe include the stiffness, yield strength and coefficient of thermal expansion. The temperature dependence of some of these properties are shown in figure 1 for aluminium alloy 6061-T6. Of interest is the region, indicated in green, where the strength and stiffness begin to decrease with temperature, as this will significantly influence the FTSI response.

To improve our ability to accurately predict the fluid-structural behaviour and fatigue lifetime of structures subjected to such high-speed flows it is necessary to develop accurate and efficient computational design tools. This requires careful validation of numerical simulations using representative experimental data sets [10]. Limited flight testing in these flow regimes from the X-15 in the 1960s to the recent flights of the X-51 and the HTV has clearly demonstrated the threat that FTSI can pose to the safe and successful operation of these vehicles. To date however there has been very limited experimental measurement of the behaviour of vehicle structures subjected to hypersonic FTSI.

We have previously established experimental techniques to investigate FSI in short-duration hypersonic wind tunnels [4,6] such as the compression-heated Ludwieg tube (TUSQ) at the University of Southern Queensland [2]. These experiments have already been used to validate a number of different numerical codes [13,16]. However, these facilities are either too low in stagnation temperature or run for insufficient flow durations to heat the models to sufficient temperatures to properly investigate thermal coupling and perform FTSI experiments. Limited testing has been performed at supersonic Mach numbers in longer duration heated wind tunnels [7] but the resultant convective model heating has been hard to control.

Bleilebens *et al.* [1] demonstrated a technique to heat a rigid compression corner model in a shock tunnel. However the long duration of pre-heating required could not produce the desired uniformity and compromised other aspects of the experiment. Kovachevich *et al.* [9] used a similar technique of internally heating metal models to investigate the influence of wall temperature on a scramjet intake. This model also suffered from long heat up times and unintentional thermal non-uniformity.

We have also recently established techniques to rapidly (<20 sec) heat wind tunnel models, both uniformly and nonuniformly, using ceramic resistance elements [15] inspired by Zander *et al.'s* use of these heaters for stagnation heating experiments [17]. We now propose a method for FTSI experiments that combines these two techniques in which a close-proximity ceramic heater is used to selectively, radiatively heat the underside of a thin compliant panel, clamped on both ends and exposed to hypersonic cross flow. This allows the FSI and FTSI response of the compliant panel to be directly compared by independently controlling the panel's temperature.

The model design would follow our previous experimental work that used thin, cantilevered, trailing-edge plates, angled to the free stream to induce a pressure differential and variously subjected to shock impingement to induce a shockwave

boundary layer interaction on the plate [4,6]. Models would be adapted to incorporate thin compliant panels, clamped at their leading and trailing edges but free along their sides, sitting above open cavities with a radiative heater located in close proximity at the base of the cavity (figure 2).

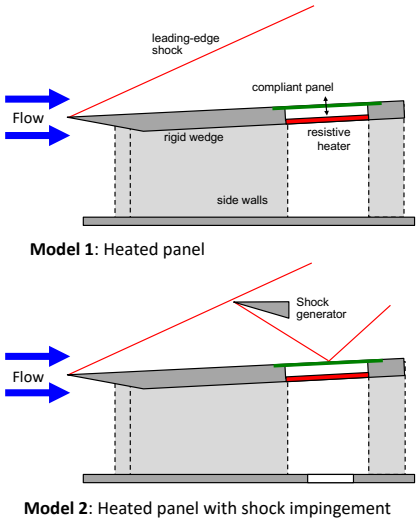

Figure 2. Schematic layouts of heated wind tunnel models for FTSI research, with and without SWBLI.

The local flow field of this nominally two-dimensional experiment is visualised using high-speed schlieren video from the side and the response of the panel is measured using both the video history and either a high-speed laser profile scanner or a digital image correlation system viewing from above the panel. IR thermography and discrete pyrometers will be used to monitor the panel surface temperature distribution, also from above the panel.

With appropriately scaled panels, using very thin gauge, these FTSI experiments could also be adapted to examine the influence of temperature on panel flutter using the approach described in [5].

Analytical Model of the Panel Heating

The system can be modelled in its simplest form as a thin metallic panel placed directly above and in line with the ceramic radiative heater with both having the same length and width (figure 2). For a given heater area (a x b) and panel material (ρ, C), the controlling parameters are therefore, the thickness of the heated panel (t), the separation between the panel and the heater (c), the operating temperature of the radiative heater (T_{rad}) and the emissivity of the heater and panel surfaces (assumed here to be the same value ε).

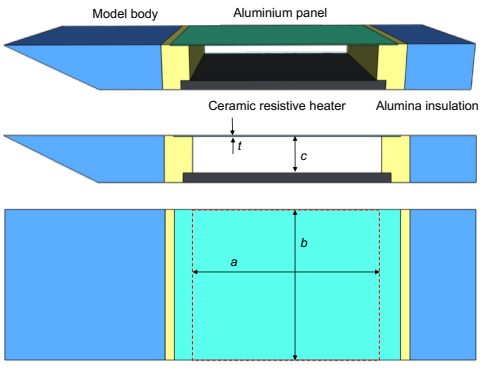

Figure 3. Schematic of simplified layout of heater and panel showing relevant dimensions for analysis.

A schematic layout of the heated model is shown in Figure 3. The ceramic resistive heater and the heated panel are thermally insulated from the rest of the model by alumina inserts. These inserts also serve to electrically insulate the resistive heater.

The net radiative flux from the heater surface to the underside of the panel is a function of the view factor. The view factor for two identical, parallel, directly opposed rectangles measuring a x b, at a separation of c, is given by [12]

$$F_{1-2} = \frac{2}{\pi XY}\left\{\ln\left[\left(\frac{(1+X^2)(1+Y^2)}{1+X^2+Y^2}\right)^{1/2}\right] + X\sqrt{1+Y^2}\tan^{-1}\frac{X}{\sqrt{1+Y^2}} + Y\sqrt{1+X^2}\tan^{-1}\frac{Y}{\sqrt{1+X^2}} - X\tan^{-1}X - Y\tan^{-1}Y\right\} \quad \text{Where } X = \frac{a}{c} \text{ and } Y = \frac{b}{c} \qquad (1)$$

It can be seen that for a pair of surfaces with aspect ratio (a/b) the view factor will decrease with separation. This decrease is more rapid for slender panels (figure 4). For surfaces measuring 100 x 80 mm, separations of less than 30 mm will ensure that at least 60% of the radiated heat is transferred to the panel. Thus, ideally the radiator should be incorporated into the model beneath the compliant panel to ensure both close proximity and minimum flow disturbance (figure 3).

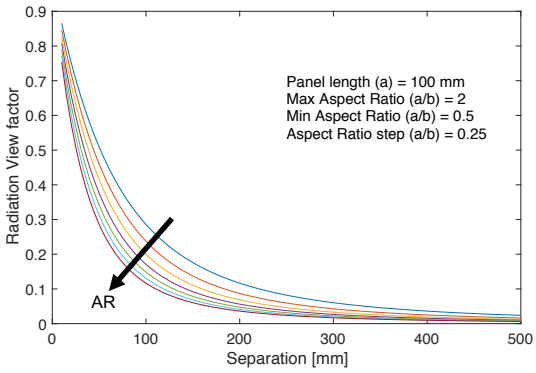

Figure 4. Variation of radiation view factor with separation, for a range of aspect ratios for surfaces of length 100 mm.

The change in temperature of the thin panel can then be calculated from

$$\Delta T = \frac{Q_{net}}{\rho(abt)C} \qquad (2)$$

Where the net heat transfer rate, Q_{net}, is the difference between the radiative input to the underside of the panel from the resistive heater and the radiative loss to the surroundings from the upper surface of the panel. This calculation models the compliant panel as a lumped mass assuming infinite conductive spread of the heat.

$$Q_{net} = Q_{rad\,in} - Q_{rad\,out}$$

$$Q_{net} = \sigma(ab)\epsilon F_{1-2}\left({T_{rad}}^4 - {T_p}^4\right) - \sigma(ab)\epsilon\left({T_p}^4 - {T_\infty}^4\right) \qquad (3)$$

The calculations reported here were performed for aluminium panels measuring 100 x 80 mm and of a range of thicknesses (t = 0.1 to 1 mm). They were heated by a similarly sized radiator, at a range of separations (c = 5 to 50 mm) and operated at a range of temperatures (500 to 1200 K). The temperature of the radiative heater is increased by increasing the electrical power passed through the ceramic radiator. Increasing the heater temperature increases the radiation adiabatic wall temperature and decreases the heating time of the compliant panel, as shown in figure 5. For higher temperatures the panel would need to be made from more thermally robust material such as titanium.

It can be seen from figure 6 that increasing the panel thickness slows the heating of the panel as it increases its thermal mass. Figure 7 shows that increasing the separation will slightly decrease both the radiation adiabatic wall temperature and the heating time. However the dependence of the panel temperature on the separation is less significant than on the heater temperature and the panel thickness for the ranges investigated.

For a 800 K radiator, a 100 x 80 x 0.5 mm aluminium panel located 20 mm above, could be heated to 640 K, it's radiation adiabatic wall temperature, in under 120 seconds. The panel will reach 500 K in 25 seconds. It would thus be necessary to heat the model immediately preceding the tunnel run.

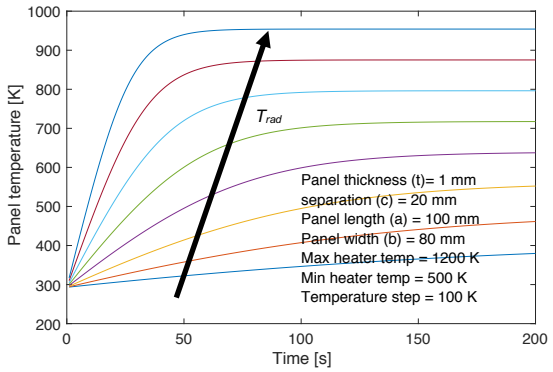

Figure 5. Panel heating history for a range of heater temperatures.

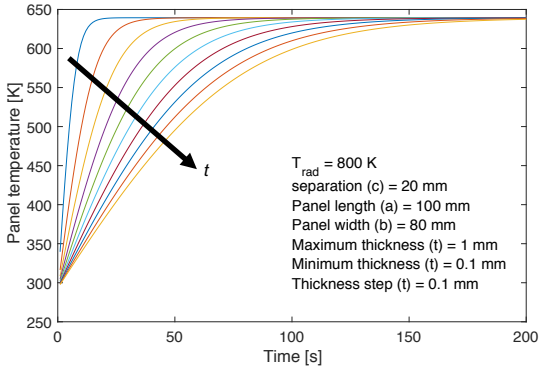

Figure 6. Panel heating history for a range of panel thicknesses.

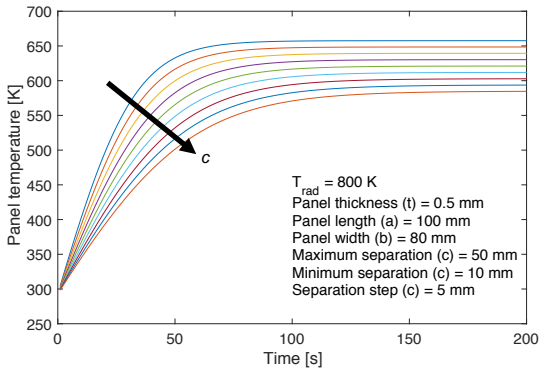

Figure 7. Panel heating history for a range of separations between the heater and the panel.

While these scenarios have been optimised to examine the FTSI behaviour of aluminium test pieces, the technique can also be used to heat materials more likely to be found in the structures of cruise vehicles, such as titanium, to representative radiation adiabatic wall temperatures of 1000+ K.

FEM Model of 3D Panel Heating

Finite element modelling (FEM) was used to validate the analytical model described above and to quantify the three-dimensionality of the heating arrangement. A 3D model was created in ANSYS Workbench incorporating the model body, alumina insulators, compliant panel and the heater plate. The heater plate was segmented into two halves so that the temperature of each could be independently varied.

The FEM model was used to first perform a simulation of uniform heating with both the heater segments run at 800 K. The result for an aluminium panel thickness of 0.5 mm and a separation of 20 mm is shown in figure 8. It can be seen that while through-thickness temperatures are uniform (within <0.5 K) in-plane thermal non-uniformity is significant. This nonuniformity is induced by the finite width of the panel and by the conduction loss to the alumina supports at the leading and trailing edges. This non-uniformity can be reduced in practice by careful design of the connection of the compliant panel to the alumina blocks and additionally by intentionally tuning the temperature distribution of the radiative heater through contouring of the resistive element [11].

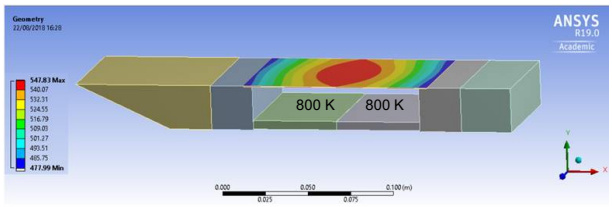

Figure 8. FEM simulation of panel temperature (0.5 mm) resulting from a uniform heater (800 K).

A second set of FEM simulations were performed on the 3D model to quantify the ability to prescribe an axially non-uniform temperature distribution on the panel. To do this, simulations were performed for a 0.5 mm aluminium panel at a range of separations (10, 20, 30, 40, 50 mm) from the radiative heater beneath it. The heater was run with the downstream segment at 800 K and the upstream segment at ambient temperature (290 K). While a discrete step is hard to achieve in practice, and not representative of the thermal gradients that would be seen on the skin of a vehicle, it provides a worst case scenario when evaluating the ability to replicate a specific temperature distribution via radiative heat transfer.

The result for an aluminium panel thickness of 0.5 mm and a separation of 20 mm is shown in figure 9. It can be seen that significant axial thermal non-uniformity is introduced by the non-uniform radiator, however, the non-uniform temperature distribution of the radiator (in this case a simple step) is significantly smeared on the panel, both by radiative cross-talk in the gap and by conduction within the panel.

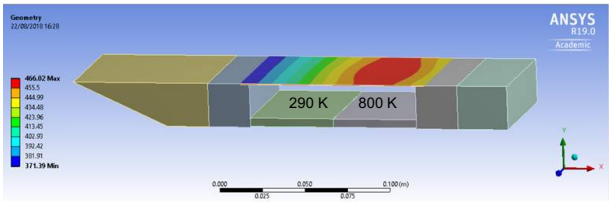

Figure 9. FEM simulation of panel (0.5 mm) temperature resulting from a non-uniform heater (290/800 K).

The axial, centreline temperature distributions on the upper surface of the panel are plotted in figure 10 for a range of separations for both the uniform and non-uniform heater cases.. It can be seen that as the separation is increased the panel

temperatures decrease, as predicted in figure 7, although the actual values are lower due to the conductive loss. The decrease in temperature with separation reduces the temperature differences driving conductive smearing, but this appears to be outweighed by an increase in smearing caused by radiative cross-talk across the enlarged gap. It is thus seen that it is difficult to preserve temperature gradients at larger separations which again motivates the inclusion of the heater at close proximity to the panel within the model.

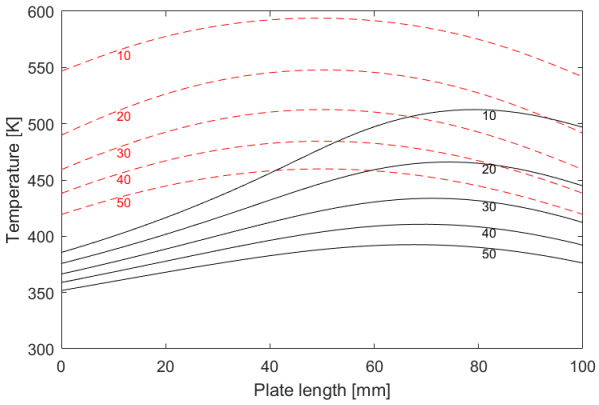

Figure 10. Surface temperature distributions along the panel centreline for a range of separations (c in mm) for both the uniform (dotted lines) and non-uniform (solid lines) heating cases.

Conclusions

Analytical predictions show that a thin, compliant clamped-clamped panel in a wind tunnel model can be heated to sufficient temperatures to induce FTSI by exposure to a close-proximity radiative heater. This heating will need to be immediately preceding an experimental run in a short-duration hypersonic wind tunnel. This radiative heater can take the form of a resistively-heated ceramic plate incorporated into the wind tunnel model and separated by a small gap (~20 mm). 3D FEM simulations show that some non-ideal non-uniformity in panel temperature will be introduced but for the range of cases examined this will be no more than 50 K for a panel heated to approximately 600 K. If it is required, a nonuniform temperature distribution can be prescribed on the compliant panel by use of a non-uniform heater, possibly using contoured resistive elements. The thermal non-uniformity of the heater will, however, be smeared on the compliant panel as a function primarily of the separation between them, but also of the panel geometry, material and the driving temperature distribution.

Acknowledgments

This work was supported by funding from the Australian Research Council (ARC-DP180103480).

References

[1] Bleilebens, M., & Olivier, H., On the Influence of. Elevated Surface Temperatures on Shock Wave/Boundary-Layer Interaction at a Heated Ramp Model. *Shock Waves, 15*, 2006, 301-312.

[2] Buttsworth, D. R., & Smart, M. K. (2010). Development of a Ludwieg Tube with Free Piston Compression Heating for Scramjet Inlet Starting Experiments, AIAA-2010-588, 2010.

[3] Culler, A. J., & McNamara, J. J., Impact of Fluid-Thermal-Structure Coupling on Response Prediction of Hypersonic Skin Panels. *AIAA Journal*, 49(11), 2393-2406

[4] Currao, G. M. D., Experimental Study of Hypersonic Fluid Structure Interaction with Shock Impingement on a Cantilever Plate. UNSW Canberra: PhD Thesis, 2018.

[5] Currao, G. M., Freydin, M., Dowell, E., McQuellin, L. P., & Neely, A. J., Design of a Panel Flutter Experiment in a Short Duration Hypersonic Facility. 21AFMC, 2018.

[6] Currao, G. M., Neely, A. J., Buttsworth, D. R., & Gai, S. L., Hypersonic Fluid-Structure Interaction on a Cantilevered Plate. 7th EUCASS. Milan, 2017.

[7] Gogulapati, A., Deshmukh, R., McNamara, J. J., Vyas, V., Wang, X., Mignolet, M. P., . . . Eason, T. G., Response of a Panel to Shock Impingement: Modeling and Comparison with Experiments - Part 2. AIAA-2015-0685, 2015.

[8] Hirschel, E.H. and Weiland, C., Design of hypersonic flight vehicles: some lessons from the past and future challenges. *CEAS Space Journal*, 1(1-4), 2011, 3-22.

[9] Kovachevich, A., Paull, A., & McIntyre, T., Investigation of an Intake Injected Hot-Wall Scramjet. AIAA-2004-1037, 2004.

[10] Matney, A., Mignolet, M. P., Culler, A. J., McNamara, J. J., & Spottswood, S. M., Panel Response Prediction Through Reduced Order Models with Application to Hypersonic Aircraft. AIAA 2015-1630, 2015.

[11] Neely, A. J., Dasgupta, A., & Choudhury, R., A New Method for Prescribing Non-Uniform Wall Temperatures on Wind Tunnel Models. 19AFMC, 2014.

[12] Siegel, R., & Howell, J. R., *Thermal Radiation Heat Transfer*. Washington: 3rd Edition, Hemisphere Publishing Corp., 1992.

[13] Sri Harsha, A., Rizwan, M., Kuldeep, S., Giridhara Prasad, A., Akhil, J., & Nagaraja, S. R., Parametric Study of Cantilever Plates Exposed to Supersonic and Hypersonic Flows. *IOP Conference Series: Materials Science and Engineering,* 2017, 1-7.

[14] Thornton, E. A., & Dechaumphai, P., Coupled Flow, Thermal and Structural Analysis of Aerodynamically Heated Panels. *Journal of Aircraft, 25*(11), 1988, 1052-1059.

[15] Vennik, J., Neely, A. J., de Baar, J. H., Tuttle, S., Choudhury, R., & Buttsworth, D. R., Reproducing Non-Uniform Surface Temperature Profiles on Hypersonic Cruise Vehicles in Impulsive Wind Tunnels. AIAA-2017-2194, 2017.

[16] Wang, L., Currao, G. M., Han, F., Neely, A. J., Young, J., & Tian, F., An immersed boundary method for fluid–structure interaction with compressible multiphase flows. *Journal of Computational Fluid Dynamics, 346*, 2017,131-151.

[17] Zander, F., Morgan, R. G., Sheikh, U., Buttsworth, D. R., & Teakle, P. R. Hot-Wall Reentry Testing in Hypersonic Impulse Facilities. *AIAA Journal, 51*(2), 2013, 476-484.

[18] MIL-HDBK-5H (1998) Metallic materials and elements for aerospace vehicle structures, US Department of Defence.